Hydrogen Formation by Proton Impact on Positronium

J. P. Merrison, H. Bluhme, J. Chevallier, B. I. Deutch,* P. Hvelplund, L. V. Jørgensen, H. Knudsen, and M. R. Poulsen
Institute of Physics and Astronomy, University of Aarhus, DK-8000 Aarhus, Denmark

M. Charlton
Department of Physics and Astronomy, University College London, Gower Street, London WC1E 6BT, United Kingdom
(Received 6 September 1996)

Hydrogen formation has been observed following proton impact on positronium. This is the first observation of charge exchange involving a positronium target. The cross section for hydrogen formation has been experimentally determined at proton energies of 11.3, 13.3, and 15.8 keV. Values of $\sigma_H = 26(\pm 9)$, $7.8(\pm 2.3)$, and $7.6(\pm 4.4) \times 10^{-16}\ \mathrm{cm}^2$ were obtained, in reasonable agreement with recent calculations. [S0031-9007(97)02936-0]

PACS numbers: 36.10.Dr, 25.43.+t, 82.55.+e

Charge exchange following proton (p^+) interaction with positronium (Ps) atoms, namely, $p^+ + \mathrm{Ps} \rightarrow H + e^+$, by which hydrogen is formed, has received considerable theoretical attention [1]. Because of the scarce nature of the Ps atoms, experimental studies involving Ps pose a considerable challenge. The motivation, for both theory and experiment, is the fundamental nature of this process, that it involves an exotic target, and also because the above reaction is the charge conjugate of an antihydrogen formation mechanism [2]. Antihydrogen has recently been observed at GeV kinetic energies in a high energy physics experiment at CERN [3]. By contrast the positronium based reaction is one of the few proposed methods [4–6] which offer the possibility to produce antihydrogen at low speeds such that it may be available for precision studies [2]. Experimental verification of the charge conjugate hydrogen formation reaction is thus a crucial test of the formation process [7].

This experiment involves colliding a proton beam at three fixed energies in the range 11–16 keV with a slow Ps target and detecting the free low energy positron liberated following electron capture [8,9]. A monoenergetic slow positron beam was utilized to create the Ps by impingement upon a heated silver foil that subsequently liberates thermally activated positronium in transmission geometry. The proton beam crosses the resulting positronium target some millimeters from the foil, and an extraction field carries the liberated free positrons through a momentum analyzer to a coincidence detection system (see Fig. 1).

The e^+ beam used for this experiment utilizes both magnetic and electrostatic transport. β^+ particles from a 1.7 GBq ^{22}Na source are moderated using a thin solid krypton film deposited onto the cryogenically cooled (7 K) source [10]. The extracted 200 eV monoenergetic beam is magnetically guided through a velocity filter before being accelerated to approximately 7.9 keV while leaving the magnetic field [8,9]. With the use of electrostatic lenses the positron beam is transported to, and focused on, a thin (2100 Å) silver foil positronium converter [11,12]. A halogen lamp is used for heating the 7 mm wide Ag foil in order to thermally desorb Ps. Since the Ag foil is held at +1900 V during operation, the positron impact energy is approximately 6 keV. At a temperature of 800 K the fraction of incident positrons thermally desorbed in transmission as orthopositronium ($\varepsilon_{\mathrm{ps}}$) has previously been determined (using a 1900 Å thick foil) to be ≈3.1% at this impact energy [12]. This fraction is the product of the 75% being implanted rather than backscattered [13], 13% transmission efficiency of the positrons to the opposite surface, 43% branching ratio for thermal desorption of Ps from the surface [14], and 75% of the Ps formed in the long lived orthostate ($^3S_1$).

A radio frequency hydrogen discharge is used to produce protons which are accelerated and focused through a 5 mm wide aperture aligned with the interaction site 4 mm from the Ag foil surface. At a proton transport energy of 17.3 keV an average current of 1.1 mA was

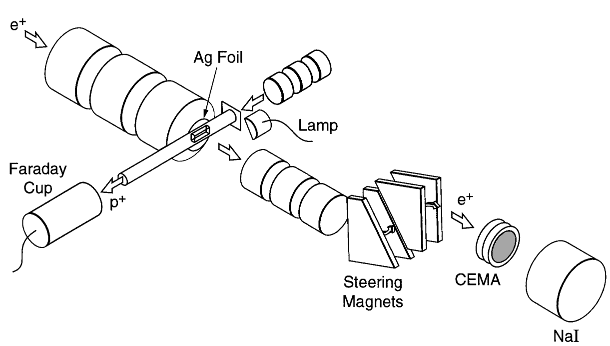

FIG. 1. A schematic of the interaction region used for detection of the residual positron following hydrogen formation via proton impact upon positronium. Positronium is thermally desorbed from a thin silver foil following positron impact. The combined effects of proton collimation and free positron energy selection determine the interaction region. The positron and proton beam lines are shown in more detail in Refs. [8] and [9].

 0031-9007/97/78(14)/2728(4)$10.00

measured by a Faraday cup placed down stream of the interaction region, and at transport energies of 14.8 and 12.8 keV the current was reduced to 1.0 and 0.72 mA, respectively. At lower transport energies the proton beam current fell rapidly due to poor focusing. The energy of the proton beam during transport was higher (by ≈ 1500 V) than while traversing the interaction region due to the electric field present there. The relative fractions of protons compared to $H_2{}^+$ and $H_3{}^+$ contained in the beam have previously been measured to be 69.0% $\pm$ 0.5%, 25.0% $\pm$ 0.5%, and 6.0% $\pm$ 0.5%, respectively, using a magnetic charge to mass analyzer in combination with a Faraday cup. It is expected that these ions behave similarly with respect to the capture process, but they introduce uncertainty in the impact velocity due to their various masses. As the presence of these ions would be expected to reduce the effective average impact velocity by only 10%, it has been neglected in this work.

Annealed tungsten meshes could be lowered in order to replace the Ag foil as the e^+ target. Slow e^+ remoderated by these meshes could be used to calibrate the extraction and detection system. The target was held at $+1520$ V and remoderated positrons were extracted through an earthed high transmission mesh before being transported (using an Einzel lens system) through a momentum selector consisting of two deflecting magnets. The e^+ were passed to a channel electron multiplier array (CEMA) and a NaI γ-ray detector which contributed the start and stop, respectively, for a time-to-amplitude converter (TAC) and multichannel analyzer (MCA) coincidence system. Calibration of this timing system allowed the resolution of the coincidence system to be determined as $210(\pm 5)$ ns with a detection efficiency (ε_{det}) of 3.9%. Preliminary results obtained at a proton impact energy of 15.8 keV utilized slightly different electronics (reduced background suppression) which had a resolution of $250(\pm 10)$ ns with a detection efficiency of 6.4%.

The extraction system was tuned to resolve positrons of 1520 eV with a FWHM of 300 eV. The extraction efficiency fell rapidly outside this energy range and had a total width of $\approx$500 eV. The target foil was 20 mm from the first (grounded) extraction lens and during data acquisition was held at $+1900$ V such that positrons liberated $4(\pm 1.5)$ mm from the Ag surface would selectively be transported to the detection system (see Fig. 1). Positrons created outside this region were assumed not to contribute to the signal. The number of positrons striking the Ag foil was determined by transporting and detecting secondary electrons liberated upon impact on the foil and performing coincidence measurements with γ-rays detected by (another) NaI detector placed close to the target area. Calibration of the γ-ray detector enabled the positron beam intensity to be integrated during data acquisition. The average beam intensity was $1.7 \times 10^6 e^+ \text{ s}^{-1}$, though for the most recent set of data obtained (while using protons at 11.3 keV impact energy) this had fallen to be $1.5 \times 10^6 e^+ \text{ s}^{-1}$. Similarly, CEMA counts were integrated and the proton beam current was monitored during data accumulation. Because of the relatively poor vacuum of the positron beam line ($\approx 10^{-8}$ Torr) the half-life of the solid krypton moderator was only $\approx$2 h such that data acquisition generally lasted only 1 hour before the moderator was replaced.

Coincidence spectra between the CEMA and γ-ray detector have been obtained, typically for 30 min, alternately with the lamp on (i.e., the Ps converter hot) and lamp off. The 210 ns time window within which positron induced events occurred was integrated over 44 hours at a proton energy of 13.3 keV. Two adjacent time windows of the same width, separated by $\sim$185 ns from the region of interest, were similarly integrated for background analysis. The averaged count rate in the region of interest was, respectively, with lamp on and lamp off 18.8 $\pm$ 0.7 and 15.9 $\pm$ 0.6 h^{-1}; the averaged background counts (over both regions) were, respectively, 14.5 $\pm$ 0.6 and 14.6 $\pm$ 0.6 h^{-1} with lamp on and lamp off. An event rate of $8.1(\pm 2.4) \times 10^{-4} \text{ s}^{-1}$ was obtained by subtracting the average count rate observed in the region of interest with the lamp off from that with the lamp on. Similarly at a proton impact energy of 11.3 keV a signal rate of $1.7(\pm 0.6) \times 10^{-3} \text{ s}^{-1}$ was obtained. Preliminary results were obtained at a proton impact energy of 15.8 keV with slightly different electronic settings, and an event rate of $1.4(\pm 0.8) \times 10^{-3} \text{ s}^{-1}$ was obtained. The total number of signal events obtained (as above) during the course of this experiment, integrated over all of these proton energies, was 211 $\pm$ 46.

There are two major sources of background which affect this experiment. One is due to random coincidences between the γ-ray detector, with a background of $\sim 40 \text{ s}^{-1}$, and the CEMA detector, which counted (at a proton impact energy of 13.3 keV) $\sim 450 \text{ s}^{-1}$ due to scattered protons and proton-induced secondary electrons. Measurements taken with the positron beam off and (alternately) lamp on and off provided coincidence count rates in the region of interest of 14.7 $\pm$ 0.7 and 15.5 $\pm$ 0.8 h^{-1}, respectively, in reasonable agreement with the expected random coincidence rate ($\sim$14 counts h^{-1}). Removing counts obtained with the lamp off from those with the lamp on (as before) produced a signal rate of $-0.8(\pm 1.1) \text{ h}^{-1}$. The second source of background arises due to the small fraction of the 6 keV positrons which penetrate the film and scatter into the combined CEMA and γ-ray detection system causing coincidences in the time window of the true signal. The positron impact energy was chosen to minimize this source of background while maintaining reasonable transmission Ps yield [12]. Similarly cosmic ray induced events may also produce coincident triggering of both detectors thereby faking a true signal. The number of events of this kind was low, coincidence integration was performed with no proton beam, but an average positron flux of 1.7×10^6 s^{-1} and event rates of 3.1 ± 0.6 and 3.8 ± 0.7 h^{-1} were obtained, respectively, with lamp on and off. The corresponding signal rate was $-0.6(\pm 0.9)$ h^{-1}.

Of the positrons reaching the transmission surface of the silver foil 43% have been observed to form Ps by thermal desorption; in addition, 29% became promptly emitted at higher energies [14]. The experimentally determined distribution of this higher energy component is broad and cuts off above 1.5 ± 0.2 eV [12]. The hydrogen formation rate due to this prompt emitted Ps may be estimated to be ≈33% of that formed by the thermally desorbed Ps component. Formation of Ps by this process is not observed to increase due to the heating of the foil. In fact some reduction occurs due to a weak temperature dependence ($\propto 1/T^{1/4}$) of the diffusion length [15]. Subsequent hydrogen formation by this Ps component will therefore not contribute to the observed signal.

A competing process to that of hydrogen formation is ionization of the positronium. This process is included in the signal (free positron detection) obtained in this experiment. The cross section for this process has been calculated using a classical (CTMC) method [16,17]. At proton impact energies below 20 keV Ps ionization is predicted to fall rapidly (see Fig. 2). At the lowest proton energy used in this study it is expected to be around an order of magnitude lower than that of hydrogen formation (obtained using the same theoretical approach) and is therefore insignificant at the level of precision achieved in this experiment.

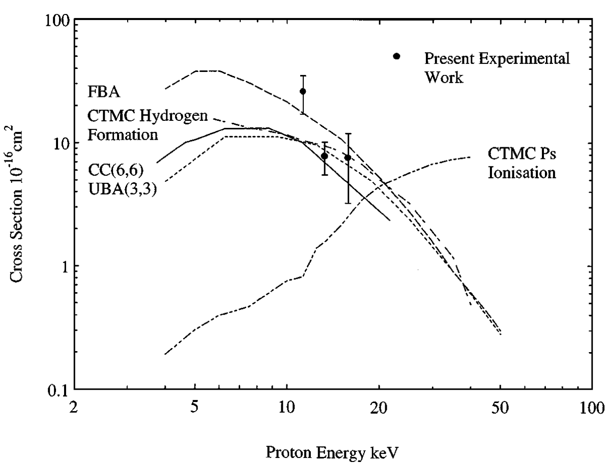

FIG. 2. Total cross sections for formation of hydrogen by proton impact upon Ps(1s). Comparison is made between the present experimental values and various theoretical approximations [1] which include the first Born approximation (FBA) [20], classical trajectory Monte Carlo (CTMC) [21], close coupling [CC(6,6)] [18,22], and the unitarized Born approximation [23]. Also shown is a (CTMC) calculation of proton-induced Ps ionization cross section [16,17] for smoothed data. Note that the statistical uncertainties have not been shown and the curve connecting the points is only to guide the eye.

The rate of detected positrons due to hydrogen formation depends not only on the measured positron and proton beam intensities (N_{e+} and I_p, respectively) and the determined detector efficiencies, but also on several geometrical properties of the experiment. The extraction system is such that only positrons liberated within a certain volume, referred to as the extracted region, are detected. This is due to the combined effects of energy and spatial resolution of the positron extraction and transport system and the proton beam collimation (see Fig. 1). An estimate must be made of the proton current passing through the extraction region as observed by the proton beam ($A_p = 3$ mm $\times$ 5 mm). Assuming a uniform distribution of protons passing through the 5 mm collimating aperture this fraction (Δ_{p+}) would be ~76%.

The extraction region as seen by the Ag foil is 5 mm $\times$ 20 mm and includes the proton beam collimation and the acceptance of the first positron transport lens. The fraction ($\Delta_{\rm Ps}$) of Ps liberated from the Ag foil which passes through this region may be estimated from knowledge of the thermally desorbed velocity distribution which has previously been experimentally determined [12]. The velocity parallel to the surface (v_s, v_y) is assumed to be Maxwell-Boltzman distributed, i.e., $N(v_{x,y}) \propto \exp(-my_{x,y}^2/kT)$, whereas in the direction perpendicular to the surface (v_z) a modified distribution of the form $N(v_z) \propto (1 + v_z^2/v_0^2)\exp(-mv_z^2/kT)$ is obtained where $v_0 = 3(\pm 2) \times 10^4$ m/s and T is the foil temperature of 800 K. The value obtained for $\Delta_{\rm Ps}$, assuming this distribution, is 78%. The average perpendicular velocity of the Ps passing through the extraction region has been determined to be 1.3×10^5 m/s. The Ps transit time across the extraction region ($\tau_{\rm ps}$) may be calculated using this velocity to be 23 ns. The fraction ($dt_{\rm ps}$) of the ($^3S_1$)Ps (of lifetime 142 ns) which survives the transit of 2.5 mm before reaching this region becomes 88%. The effective Ps density may be obtained from these combined values, bracketed in the equation below. This expression includes these factors to determine the hydrogen formation cross section from the detected positron count rate ($N_{\rm Hdet}$).

$$\sigma_{\rm H} = N_{\rm Hdet}A_p/(N_{e+}\{\varepsilon_{\rm ps}\tau_{\rm ps}dt_{\rm ps}\Delta_{\rm ps}\}\,\varepsilon_{\rm det}I_p\Delta_{p+})\,.$$

The data presented provide values for the hydrogen formation cross section of $\sigma_{\rm H} = 26(\pm 9)$, $7.8(\pm 2.3)$, and $7.6(\pm 4.4) \times 10^{-16}$ cm^2 at proton impact energies of 11.3, 13.3, and 15.8 keV, respectively. These experimentally determined values are plotted in Fig. 2 together with various recent calculations of the hydrogen formation cross section for proton-Ps collision. Reasonable agreement between experiment and theory is achieved with calculated values lying in the region $\sigma_{\rm H} \approx (5-20) \times 10^{-16}$ cm^2 at these proton impact energies. The calculations involved various theoretical approaches [1], and the most accurate are considered to be those using the close-coupling technique [CC(6,6)], though these do not include formation of hydrogen in states greater than $n = 2$ and therefore constitute a lower estimate [18].

The general agreement between our experimental data and the theoretical results demonstrates the ability of theorists to treat charge exchange reactions involving the special Ps target. The present experimental demonstration of hydrogen formation via proton-positronium impact is furthermore supportive for the production of antihydrogen using this reaction. In the proton rest frame these experimental results correspond to positronium energies of 12–17 eV, close to the peak energy observed for Ps backscattering due to low energy positron impact upon metal surfaces [19]. These measured cross sections may thus be applied to positronium interaction with trapped antiprotons.

We wish to acknowledge the invaluable support of Poul Aggerholm, the help of Gaetana Laricchia and Finn Jacobsen in the early stages of the experiment, and the useful discussions with Alexei Ermolaev and Jim Mitroy. Also the financial support from the SERC (U.K.), from the Danish Research Academy, and to J.M. from the EC Human Capital and Mobility Program is acknowledged.

*Deceased.

[1] A.M. Ermolaev, Hyperfine Interact. **100**, 41 (1996).
[2] M. Charlton, J. Eades, D. Horváth, R.J. Hughes, and C. Zimmermann, Phys. Rep. **241**, 65 (1994).
[3] G. Baur, G. Boero, S. Brauksiepe, A. Buzzo, W. Eyrich, R. Geyer, D. Grzonka, J. Hauffe, K. Kilian, M. LoVetere, M. Macri, M. Moosburger, R. Nellen, W. Oelert, S. Passaggio, A. Pozzo, K. Röhrich, K. Sachs, G. Schepers, T. Sefzick, R.S. Simon, R. Stratmann, F. Stinzing, and M. Wolke, Phys. Lett. B **368**, 251 (1996).
[4] G. Gabrielse, S. Rolston, L. Haarsma, and W. Kells, Phys. Lett. A **129**, 38 (1988).
[5] J. Walz, S.B. Ross, C. Zimmermann, L. Ricci, M. Prevedelli, and T.W. Hänsch, Phys. Rev. Lett. **75**, 3527 (1995).
[6] B.I. Deutch, A.S. Jensen, A. Miranda, and G.C. Oades, in Proceedings of the 1st Workshop on Antimatter Physics at Low Energies (FNAL, Batavia, IL, 1986), p. 371.
[7] J.W. Humberston, M. Charlton, F.M. Jacobsen, and B.I. Deutch, J. Phys. B **20**, L25 (1987).
[8] B.I. Deutch, Mater. Sci. Forum **175–178**, 21 (1995).
[9] J.P. Merrison, Hyperfine Interact. **100**, 65 (1996).
[10] J.P. Merrison, M. Charlton, B.I. Deutch, and L.V. Jørgensen, Hyperfine Interact. **76**, 305 (1993).
[11] M.R. Poulsen, M. Charlton, J. Chevallier, B.I. Deutch, L.V. Jørgensen, and G. Laricchia, J. Phys. Condens. Matter **3**, 2849 (1991).
[12] M.R. Poulsen, M. Charlton, B.I. Deutch, L.V. Jørgensen, and G. Laricchia, Hyperfine Interact. **76**, 309 (1993).
[13] P.G. Coleman, L. Albrecht, K.O. Jensen, and A.B. Walker, J. Phys. Condens. Matter **4**, 10 311 (1992).
[14] K.G. Lynn and D.O. Welch, Phys. Rev. B **22**, 99 (1980).
[15] E. Soininen, H. Huomo, P.A. Huttunen, J. Mäkinen, A. Vehanen, and P. Hautojärvi, Phys. Rev. B **41**, 6227 (1989).
[16] A.M. Ermolaev, B.H. Bransden, and C.R. Mandal, Phys. Lett. A **125**, 44 (1987).
[17] A.M. Ermolaev (private communication).
[18] J. Mitroy and K. Ratnavelu, J. Phys. B **28**, 287 (1995).
[19] R.H. Howell, I.J. Rosenberg, and M.J. Fluss, Phys. Rev. B **34**, 3069 (1986).
[20] J.W. Darewych, J. Phys. B **20**, 5917 (1987).
[21] A.M. Ermolaev, Hyperfine Interact. **44**, 375 (1988).
[22] J. Mitroy and A.T. Stelbovics, J. Phys. B **27**, L55 (1994).
[23] J. Mitroy and A.T. Stelbovics, Phys. Rev. Lett. **72**, 3495 (1994).